

## Exotic magnetism in the alkali sesquioxides $\text{Rb}_4\text{O}_6$ and $\text{Cs}_4\text{O}_6$

Jürgen Winterlik, Gerhard H. Fecher, Taras Palasyuk, Claudia Felser

*Institute for Inorganic and Analytic Chemistry,*

*Johannes Gutenberg - Universität, D-55099 Mainz, Germany.*

Jürgen Kübler

*Institute for Solid State Physics, Technische Universität, 64289 Darmstadt, Germany*

Claus Mühle, Martin Jansen

*Max - Planck - Institute for Solid State Research, 70569 Stuttgart, Germany*

Ivan Trojan, Sergey Medvedev, Mikhail I. Erements

*Max - Planck - Institute for Chemistry, 55020 Mainz, Germany*

Franziska Emmerling

*Bundesanstalt Materialforschung und Prüfung Berlin, 12489 Berlin, Germany*

(Dated: October 29, 2018)

## Abstract

Among the various alkali oxides the sesquioxides  $\text{Rb}_4\text{O}_6$  and  $\text{Cs}_4\text{O}_6$  are of special interest. Electronic structure calculations using the local spin-density approximation predicted that  $\text{Rb}_4\text{O}_6$  should be a half-metallic ferromagnet, which was later contradicted when an experimental investigation of the temperature dependent magnetization of  $\text{Rb}_4\text{O}_6$  showed a low-temperature magnetic transition and differences between zero-field-cooled (ZFC) and field-cooled (FC) measurements. Such behavior is known from spin glasses and frustrated systems.  $\text{Rb}_4\text{O}_6$  and  $\text{Cs}_4\text{O}_6$  comprise two different types of dioxygen anions, the hyperoxide and the peroxide anions. The nonmagnetic peroxide anions do not contain unpaired electrons while the hyperoxide anions contain unpaired electrons in antibonding  $\pi^*$ -orbitals. High electron localization (narrow bands) suggests that electronic correlations are of major importance in these open shell  $p$ -electron systems. Correlations and charge ordering due to the mixed valency render  $p$ -electron-based anionogenic magnetic order possible in the sesquioxides. In this work we present an experimental comparison of  $\text{Rb}_4\text{O}_6$  and the related  $\text{Cs}_4\text{O}_6$ . The crystal structures are verified using powder x-ray diffraction. The mixed valency of both compounds is confirmed using Raman spectroscopy, and time-dependent magnetization experiments indicate that both compounds show magnetic frustration, a feature only previously known from  $d$ - and  $f$ -electron systems.

PACS numbers: 71.20.Be, 75.50.-y, 68.47.Gh

Keywords: Open shell systems, Oxides, Magnetism, Electronic structure

## I. INTRODUCTION

Magnetism arising from  $d$ - and  $f$ -shells has drawn the bulk of research attention but  $p$ -electron based magnetic order is a rare and fascinating topic that presents the added challenge of molecular and not just atomic ordering. The majority of main group molecules are nonmagnetic. Few exceptions are found, e.g. in NO, NO<sub>2</sub> and O<sub>2</sub>. Molecular oxygen contains two single electrons in degenerate antibonding  $\pi^*$ -orbitals, which can order magnetically in a solid crystal. Solid oxygen shows a large variety of magnetic phenomena ranging from antiferromagnetism to superconductivity.<sup>1,2,3,4,5</sup>

What applies to molecular oxygen applies equally to charged oxygen molecules with unpaired electrons. Dioxygen anions are principally found in alkali and alkaline earth oxides, which represent excellent model systems because of their supposedly simple electron configurations. The hyperoxide anion O<sub>2</sub><sup>-</sup> corresponds to "charged oxygen". Since it still contains one unpaired electron, magnetic order is enabled for hyperoxides. KO<sub>2</sub>, RbO<sub>2</sub>, and CsO<sub>2</sub> are known to exhibit antiferromagnetic ordering below their respective Néel temperatures of 7 K, 15 K, and 9.6 K, respectively.<sup>6,7</sup>

Among the alkali oxides, the sesquioxides are of special interest. In contrast to related compounds, which are white, yellow, or orange, the sesquioxides Rb<sub>4</sub>O<sub>6</sub> and Cs<sub>4</sub>O<sub>6</sub> are black. Furthermore, a formula unit AM<sub>4</sub>O<sub>6</sub> (AM = alkali metals Rb or Cs) contains two different types of dioxygen anions: one closed-shell nonmagnetic peroxide anion and two of the aforementioned hyperoxide anions. The structural formula of the sesquioxides is thus accurately represented as (AM<sup>+</sup>)<sub>4</sub>(O<sub>2</sub><sup>-</sup>)<sub>2</sub>(O<sub>2</sub><sup>2-</sup>).<sup>8</sup> The mixed valency enables complicated magnetic structures in the sesquioxides. The first descriptions of the crystal structures of the sesquioxides were published in 1939 in the pioneering works of Helms and Klemm.<sup>9,10,11</sup> Both compounds belong to the Pu<sub>2</sub>C<sub>3</sub> structure type and to space group  $I\bar{4}3d$ . This Pu<sub>2</sub>C<sub>3</sub> structure type is known from the noncentrosymmetric rare earth metal sesquicarbide superconductors such as Y<sub>2</sub>C<sub>3</sub> with a maximum critical temperature of  $T_c = 18$  K.<sup>12</sup> For Cs<sub>4</sub>O<sub>6</sub>, the literature runs out after 1939 because of the extremely challenging synthesis and sensitivity to air. In Rb<sub>4</sub>O<sub>6</sub>, the presence of both peroxide and hyperoxide anions was verified by neutron scattering<sup>13</sup>, and electronic structure calculations using the local spin density approximation (LSDA) were performed to explain the exceptional black color.<sup>14</sup> These same calculations predicted a half-metallic ferromagnetic ground state but were contradicted by

later experiments in which a transition was found to occur at approximately 3.4 K in the temperature dependent magnetization.<sup>15</sup> Differences between ZFC and FC measurements indicated that  $\text{Rb}_4\text{O}_6$  behaves like a frustrated system or a spin glass. Recently published electronic structure calculations are consistent with the experimental findings.<sup>16</sup> It was shown that for an accurate theoretical treatment of highly localized systems such as  $\text{Rb}_4\text{O}_6$  and  $\text{Cs}_4\text{O}_6$ , a symmetry reduction, exact exchange and electron-electron correlations have to be considered in the calculations. This can be generalized to any other open shell system that is based on  $p$ -electrons. Accounting for these features the calculations result in an insulating ground state. Further calculations using the spin spiral method show that  $\text{Rb}_4\text{O}_6$  exhibits spin spiral behavior in a certain crystal direction. The energy changes are extremely small along this direction indicating a multidegenerate ground state.<sup>16</sup> In this work we present the routes of synthesis for  $\text{Rb}_4\text{O}_6$  and  $\text{Cs}_4\text{O}_6$  and the structural verification using powder x-ray diffraction (XRD). Raman spectroscopic measurements confirm the mixed valency of the used  $\text{Rb}_4\text{O}_6$  and  $\text{Cs}_4\text{O}_6$  samples. Magnetization experiments are shown that indicate a dynamic time dependent magnetism of  $\text{Rb}_4\text{O}_6$ . Furthermore we present a comprehensive experimental study of  $\text{Cs}_4\text{O}_6$ , which has not been extensively investigated due to the difficulty of sample preparation. Magnetization measurements dependent on temperature, magnetic field, and time provide evidence that  $\text{Cs}_4\text{O}_6$  shows a similar behavior as  $\text{Rb}_4\text{O}_6$ . According to experimental and theoretical investigations,<sup>16</sup> both sesquioxides are mixed valent highly correlated systems exhibiting  $p$ -electron based magnetic frustration. These seemingly simple compounds can serve as model systems for any other open-shell systems that are based on  $p$ -electrons such as hole-doped  $\text{MgO}$ <sup>17</sup> or nanographene.<sup>18</sup>

## II. STRUCTURE

Figure 1 depicts a body-centered cubic unit cell of  $\text{AM}_4\text{O}_6$ . The 24 oxygen atoms in the cubic cell form 12 molecules that can be distinguished both by their valency and by their alignment along the principal axes. We assumed the nonmagnetic peroxide anions to be oriented along the  $z$ -axis, whereas the hyperoxides are oriented along the  $x$ - and  $y$ -axes. The experimental bond lengths for the hyperoxide and the peroxide anions are  $0.144 a$  and  $0.165 a$ , respectively<sup>19,20</sup>. The cubic lattice parameters are found in Section IV.

### III. SYNTHESIS

The precursors rubidium and cesium oxide  $AM_2O$  as well as rubidium and cesium hyperoxide  $AMO_2$  were prepared from elemental sources. For  $AM_2O$ , liquid rubidium/cesium, purified by distillation, was reacted with a stoichiometric amount of dry oxygen in an evacuated glass tube followed by heating at 473 K for two weeks under argon atmosphere.<sup>21,22</sup> The samples were subsequently ground under argon and the entire cycle was repeated five times. A slight excess of rubidium/cesium was distilled at 573 K in vacuum, resulting in a pale green powder of  $Rb_2O$  and an orange powder of  $Cs_2O$ .  $AMO_2$  were prepared through the reaction of liquid rubidium/cesium and an excess of dry oxygen using the same method as described for  $AM_2O$ , resulting in yellow powders of  $RbO_2$  and  $CsO_2$ , respectively.

$Rb_4O_6$  was obtained by a solid state reaction of 400 mg  $RbO_2$  and 160 mg  $Rb_2O$  in a molecular ratio of 4 : 1 in a glass tube sealed under argon at 453 K for 24 hours.  $Cs_4O_6$  was obtained in the same way using the amounts of 468 mg  $CsO_2$  and 280 mg  $Cs_2O$  and annealing at 473 K for 24 hours. For the reaction, a slight excess of  $Cs_2O$  was used to compensate for small amounts of cesium peroxide, which is always contained as an impurity in  $Cs_2O$ . The very air sensitive products were ground and the reaction was repeated until pure phases were obtained (black powders). For the magnetization measurements,  $Rb_4O_6$  and  $Cs_4O_6$  were sealed in a high-purity quartz tube (Suprasil glass) under helium atmosphere.

### IV. STRUCTURAL CHARACTERIZATION

The crystal structures of the compounds were investigated using XRD. The measurements were carried out using a Bruker D8 diffractometer with Cu  $K_{\alpha 1}$  radiation for  $Rb_4O_6$  and Mo  $K_{\alpha 1}$  for  $Cs_4O_6$ . The samples were measured in sealed capillary tubes under an argon atmosphere. The diffraction patterns are shown in Figure 2. The raw data (black) are compared to the difference between a calculated Rietveld refinement and the raw data (gray). The refinements yielded weighted profile R-values of  $R_{wp} = 8.216$  for  $Rb_4O_6$  and 6.388 for  $Cs_4O_6$ . Both compounds crystallize in the cubic structure  $I\bar{4}3d$  (space group 220). The experimental lattice parameters as found from Rietveld refinements are 9.322649(74) Å for  $Rb_4O_6$  and 9.84583(11) Å for  $Cs_4O_6$ . The atomic parameters for both compounds are shown in Table I, additional structural information is found in Table II. The pattern of  $Rb_4O_6$

indicates good phase purity. In the case of  $\text{Cs}_4\text{O}_6$ , additional signals were detected. The signals were identified to arise from the impurity  $\text{CsO}_2$ , which belongs to the cubic space group  $Fm\bar{3}m$  and has a lattice parameter of  $a = 6.55296(37)$  Å. The impurity phase was included in the refinement of  $\text{Cs}_4\text{O}_6$ . An impurity content of approximately 7.23% of  $\text{CsO}_2$  in  $\text{Cs}_4\text{O}_6$  was derived from the refinement.

## V. RAMAN SPECTROSCOPY

The presence of peroxide and hyperoxide anions in  $\text{Rb}_4\text{O}_6$  and  $\text{Cs}_4\text{O}_6$  was verified using Raman spectroscopy. The measurements were performed using a diamond anvil cell (DAC) in order to prevent sample decomposition from contact with air and moisture. The samples were loaded in a dry box under dry nitrogen atmosphere. The samples were confined within a cylindrical hole of 100 microns diameter and 50 microns height drilled in a Re gasket. We used synthetic type-IIa diamond anvils, which have only traces of impurities ( $<1$  ppm) and very low intrinsic luminescence. Raman spectra were recorded with a single 460-mm-focal-length imaging spectrometer (Jobin Yvon HR 460) equipped with 900 and 150 grooves/mm gratings, giving a resolution of  $15\text{ cm}^{-1}$ , notch-filter (Kaiser Optics), liquid nitrogen cooled charge-coupled device (CCD (Roper Scientific)). Scattering calibration was done using Ne lines with an uncertainty of  $\pm 1\text{ cm}^{-1}$ . The He-Ne laser of Melles Griot with the wavelength of 632.817 nm was used for excitation of the sample. The probing area was a spot with 5 microns diameter. Figure 3 shows the Raman spectrum of  $\text{Rb}_4\text{O}_6$  in a range from 700-1250  $\text{cm}^{-1}$ . Two peaks are found at Raman shifts of 795  $\text{cm}^{-1}$  and 1153  $\text{cm}^{-1}$ , respectively. The signal at 795  $\text{cm}^{-1}$  corresponds to the stretching vibration of the peroxide anions and is in good agreement with the literature value of 782  $\text{cm}^{-1}$  for  $\text{Rb}_2\text{O}_2$ .<sup>23</sup> The peak at 1153  $\text{cm}^{-1}$  is assigned to the corresponding vibration of the hyperoxide anions and comparable to the literature value of 1140  $\text{cm}^{-1}$  for  $\text{RbO}_2$ .<sup>24</sup> In the Raman spectrum for  $\text{Cs}_4\text{O}_6$ , which was recorded as described above, signals of 738  $\text{cm}^{-1}$  and 1128  $\text{cm}^{-1}$  were recorded. The simultaneous presence of both dioxygen anion types and thus the mixed valency is proven for both  $\text{Rb}_4\text{O}_6$  and  $\text{Cs}_4\text{O}_6$ .

## VI. MAGNETIZATION

The magnetic properties of  $\text{Rb}_4\text{O}_6$  and  $\text{Cs}_4\text{O}_6$  were investigated using a superconducting quantum interference device (SQUID, Quantum Design MPMS-XL5). Samples of approximately 100 mg, fused in Suprasil tubes under helium atmosphere, were used for the analysis. In the cases of temperature dependent and time dependent magnetometry we performed under zero-field-cooled (ZFC) and field-cooled (FC) measurements. For the ZFC conditions, the samples were first cooled to a temperature of 1.8 K without applying a magnetic field. After applying an induction field  $\mu_0 H$ , the magnetization was recorded as a function of temperature or time. For the temperature dependent measurements, the magnetization was recorded directly afterward in the same field upon lowering the temperature down to 1.8 K again (FC).

Temperature dependent magnetization experiments were discussed in an earlier work<sup>15</sup> and indicate that  $\text{Rb}_4\text{O}_6$  behaves like a frustrated system. We have analyzed the related  $\text{Cs}_4\text{O}_6$  using an identical experimental setup. Figures 4(a) and (b) display the temperature dependent magnetization of  $\text{Cs}_4\text{O}_6$  at magnetic induction fields  $\mu_0 H$  of 2 mT and 5 T, respectively. The measurements were carried out under ZFC conditions and FC conditions. In the 2 mT ZFC measurement, a magnetic transition is found to occur at  $3.2 \pm 0.2$  K. In the 5 T ZFC curve, this transition shows a distinct broadening and is shifted to a higher temperature. Thermal irreversibilities between ZFC and FC measurements are observed in both magnetic fields, a behavior known from frustrated systems and spin glasses.  $\text{Cs}_4\text{O}_6$  exhibits similar magnetic properties as  $\text{Rb}_4\text{O}_6$ .

Figure 5 shows Curie-Weiss-Fits of  $\text{Rb}_4\text{O}_6$  and  $\text{Cs}_4\text{O}_6$  in temperature ranges of 100-300 K at magnetic fields of 5 T. The fits were performed in the region above 200 K and yield negative paramagnetic transition temperatures for both compounds ( $\Theta_D = -6.9$  K for  $\text{Rb}_4\text{O}_6$ <sup>15</sup> and  $\Theta_D = -4.5$  K for  $\text{Cs}_4\text{O}_6$ ). This indicates dominance of antiferromagnetic interactions. From the high temperature data, an effective magnetic moment of  $m = 1.83\mu_B$  per hyperoxide anion can be deduced applying the Curie-Weiss law based on molecular field theory (MFT) for  $\text{Rb}_4\text{O}_6$ , whereas the moment was calculated to amount to  $m = 2.01\mu_B$  for  $\text{Cs}_4\text{O}_6$ . These values are in modest agreement with  $1.73\mu_B$  as expected from MFT using the spin-only approximation. The inverse susceptibility of  $\text{Cs}_4\text{O}_6$  exhibits a broad peak at approximately 210 K. The origin of this peak is not clear. Several alkali oxides are, however, known to

show multiple phase transitions,<sup>7,25</sup> which are in some cases even very small changes of the lattice parameters. The peak may correspond to such a phase transition.

We also performed field-dependent magnetization measurements. Figure 6(a) shows the field dependent magnetization of  $\text{Rb}_4\text{O}_6$  at 2 K, well below the magnetic transition temperature of 3.4 K. It is clear that the magnetization does not show hysteresis [see inset (i)]. The shape of the magnetization curve is best modelled by a paramagnetic loop correction to a Langevin function  $L(H)$  given by  $M(H) = \chi_{lin}H + M_0L(H)$ , where  $\chi_{lin}$  is the field independent paramagnetic susceptibility and  $M_0$  the saturation moment. In inset (ii), the linear contribution was subtracted from the total magnetization. The remaining Langevin function saturates initially with a magnetic moment of  $0.25 \mu_B$  per  $\text{Rb}_4\text{O}_6$  formula unit and increases in successive cycles. At given magnetic fields, the up and down curves exhibit differences in the measured magnetization, indicating that the magnetization changes with time in a manner consistent with the known relaxation behavior of frustrated systems.<sup>26</sup> Figure 6(b) shows the corresponding field dependent magnetization for  $\text{Cs}_4\text{O}_6$ , qualitatively similar to  $\text{Rb}_4\text{O}_6$ . Applying the model of the paramagnetic loop correction to a Langevin function as described above a saturation magnetic moment of  $0.37 \mu_B$  per  $\text{Cs}_4\text{O}_6$  formula unit is obtained as seen in Figure 6(b) inset (ii). While the total magnetic moments of  $\text{Rb}_4\text{O}_6$  and  $\text{Cs}_4\text{O}_6$  are quite similar at given magnetic fields, the paramagnetic contributions exhibit a large difference. This indicates that the time dependence and the dynamics of the compounds are differing.

Time dependent measurements reveal more about these dynamics. Figures 7(a) and (b) show the time dependent variations of the magnetization up to 6400 s for both compounds. The measurements were performed under ZFC conditions at 2 K in induction fields of 1 T. The magnetic moment of  $\text{Rb}_4\text{O}_6$  varies exponentially with a relaxation time of  $\tau = (1852 \pm 30)$  s. This value is comparable to those of other frustrated systems. Similar curves were obtained for  $\text{Rb}_4\text{O}_6$  using lower as well as higher induction fields of 30 mT and 5 T. The relaxation times were determined to be  $\tau(30 \text{ mT}) = (1170 \pm 30)$  s and  $\tau(5 \text{ T}) = (4340 \pm 20)$  s. The pronounced relaxation is another clear indication of the magnetic frustration in  $\text{Rb}_4\text{O}_6$ .

As in the case of  $\text{Rb}_4\text{O}_6$ , the magnetic moment of  $\text{Cs}_4\text{O}_6$  follows exponential behavior. A relaxation time of  $\tau = (3701 \pm 30)$  s is deduced from the exponential fit confirming that  $\text{Cs}_4\text{O}_6$  is also a magnetically frustrated  $2p$ -system although with different dynamics. The fitting curve does not follow the exponential behavior as exactly as for  $\text{Rb}_4\text{O}_6$ . This is most



probably due to the fact that a complete saturation of the magnetization is not reached within the time span of 6400 s. A reason for these differences between the compounds cannot be given within the scope of these experiments, but electronic structure calculations for  $\text{Cs}_4\text{O}_6$  may shed more light on the dynamics of this system.

## VII. SUMMARY AND CONCLUSIONS

It has been shown that the alkali sesquioxides  $\text{Rb}_4\text{O}_6$  and  $\text{Cs}_4\text{O}_6$  exhibit frustrated magnetic ordering based on anionogenic  $2p$ -electrons of the hyperoxide anions. Mixed valency was verified in both compounds using Raman spectroscopy. The strong time dependence of the magnetization and the pronounced differences between the ZFC and FC measurements support the previously assumed frustrated state of  $\text{Rb}_4\text{O}_6$ <sup>16</sup>.  $\text{Cs}_4\text{O}_6$  was found to show a very similar behavior. The experiments show that strong electronic correlations can also occur in presumably simple  $2p$ -compounds such as alkali oxides. The complex distribution of magnetic moments in the lattices leads to a symmetry reduction and causes a frustrated magnetic behavior in both compounds. These results are of major importance since they confirm that open shell  $p$ -electrons can behave like  $d$ - or  $f$ -electrons.

### Acknowledgments

This work was funded by the DFG in the Collaborative Research Center *Condensed Matter Systems with Variable Many-Body Interactions* (TRR 49). The authors are grateful for the fruitful discussions with W. Pickett, M. Jourdan, G. Jakob and H. von Löhneysen. T. P.<sup>1</sup>, I. T.<sup>2</sup> and S. M.<sup>3</sup> thank their home institutes for support (<sup>1</sup> Institute of Physical Chemistry PAS, Kasprzaka 44/52, 01-224 Warsaw, Poland, <sup>2</sup> A. V. Shubnikov Institute of Crystallography, RAS, 117333, Leninskii pr.59, Moscow, Russia, and <sup>3</sup> National Technical University "KhPI", Frunze Str. 21, 61002 Kharkov, Ukraine)

---

<sup>1</sup> Y. A. Freiman and H. J. Jodl, Phys. Reports **401**, 1 (2004).

<sup>2</sup> R. B. Meier and R. B. Helmholtz, Phys. Rev. B **29**, 1387 (1984).

<sup>3</sup> I. N. Goncharenko, O. L. Makarova, and L. Ulivi, Phys. Rev. Lett. **93**, 055502 (2004).

- <sup>4</sup> Y. Akahama, H. Kawamura, D. Husermann, M. Hanfland, and O. Shimomura, *Phys. Rev. Lett.* **74**, 4690 (1995).
- <sup>5</sup> K. Shimizu, K. Suhara, M. Ikumo, M. I. Erements, and K. Amaya, *Nature* **393**, 767 (1998).
- <sup>6</sup> M. Labhart, D. Raoux, W. Känzig, and M. A. Bösch, *Phys. Rev. B* **20**, 53 (1979).
- <sup>7</sup> W. Hesse, M. Jansen, and W. Schnick, *Prog. Solid State Chem.* **19**, 47 (1989).
- <sup>8</sup> M. Jansen and N. Korber, *Z. Anorg. Allg. Chemie* **598/599**, 163 (1991).
- <sup>9</sup> A. Helms and W. Klemm, *Z. Anorg. Allg. Chemie* **242**, 33 (1939).
- <sup>10</sup> A. Helms and W. Klemm, *Z. Anorg. Allg. Chemie* **242**, 97 (1939).
- <sup>11</sup> A. Helms and W. Klemm, *Z. Anorg. Allg. Chemie* **242**, 201 (1939).
- <sup>12</sup> S. Kuroiwa, Y. Saura, J. Akimitsu, M. Hiraishi, M. Miyazaki, K. H. Satoh, S. Takeshita, and R. Kadono, *Phys. Rev. Lett.* **100**, 097002 (2008).
- <sup>13</sup> M. Jansen, R. Hagenmayer, and N. Korber, *C. R. Acad. Sci. Ser. IIc: Chim.* p. 591 (1999).
- <sup>14</sup> J. J. Attema, G. A. de Wijs, G. R. Blake, and R. A. de Groot, *J. Am. Chem. Soc.* **127**, 16325 (2005).
- <sup>15</sup> J. Winterlik, G. H. Fecher, and C. Felser, *J. Am. Chem. Soc.* **129**, 6990 (2007).
- <sup>16</sup> J. Winterlik, G. H. Fecher, C. A. Jenkins, C. Felser, C. Mühle, K. Doll, M. Jansen, L. M. Sandratskii, and J. Kübler, *Phys. Rev. Lett.* **102**, 016401 (2009).
- <sup>17</sup> I. S. Elfimov, A. Rusydi, S. I. Csiszar, Z. Hu, H. H. Hsieh, H.-J. Lin, C. T. Chen, R. Liang, and G. A. Sawatzky, *Phys. Rev. Lett.* **98**, 137202 (2007).
- <sup>18</sup> Y.-W. Son, M. L. Cohen, and S. G. Louie, *Nature* **444**, 347 (2006).
- <sup>19</sup> T. Bremm and M. Jansen, *Z. Anorg. Allg. Chemie* **610**, 64 (1992).
- <sup>20</sup> H. Seyeda and M. Jansen, *J. Chem. Soc. Dalton Trans.* p. 875 (1998).
- <sup>21</sup> L. Hackspill, *Helv. Chim. Acta* **11**, 1008 (1928).
- <sup>22</sup> G. Brauer, *Handbuch der Präparativen Anorganischen Chemie*, vol. 2 (Enke-Verlag Stuttgart, Germany, 1978).
- <sup>23</sup> H. H. Eysel and S. Thym, *Z. anorg. allg. Chem.* **411**, 97 (1975).
- <sup>24</sup> J. B. Bates, M. H. Brooker, and G. E. Boyd, *Chem. Phys. Lett.* **16**, 391 (1972).
- <sup>25</sup> M. Rosenfeld, M. Ziegler, and W. Känzig, *Helv. Phys. Acta* **51**, 298 (1978).
- <sup>26</sup> J. Schmalian and P. G. Wolynes, *Phys. Rev. Lett.* **85**, 836 (2000).

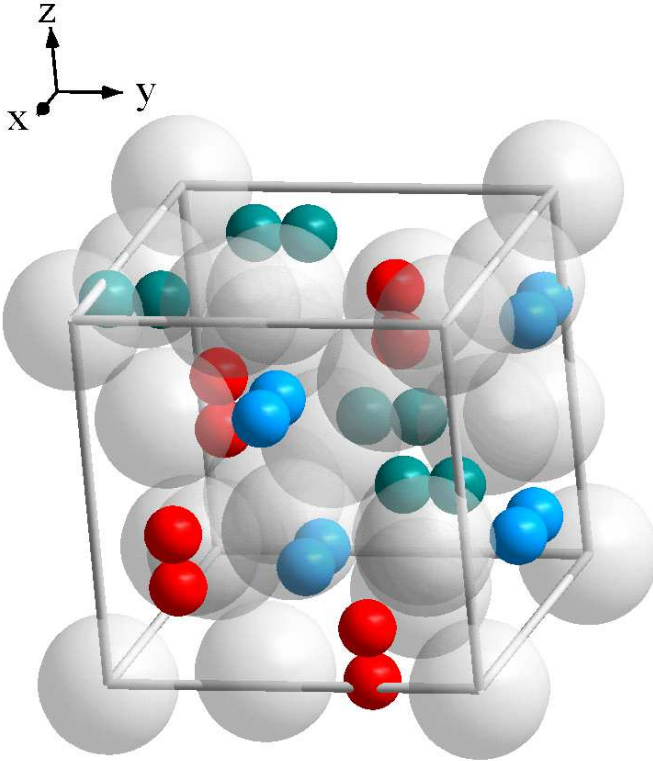


FIG. 1: (Color online) Pseudo-body-centered cubic cell of the alkali sesquioxides  $AM_4O_6$  ( $AM = Rb, Cs$ ). Differently oriented dioxygen anions are drawn with different colors so that the alignment along the axes can be distinguished. For clarity, the Rb/Cs atoms are gray and transparent.

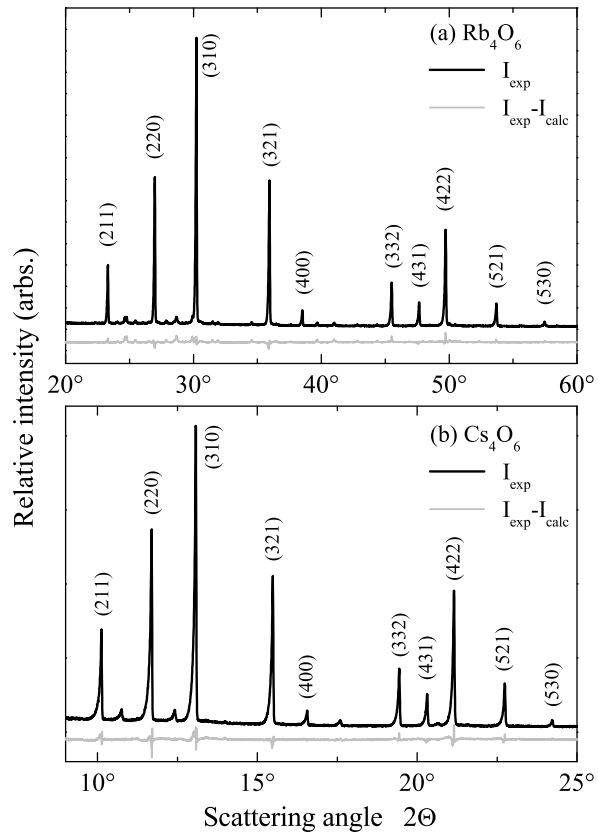


FIG. 2: Powder x-ray diffraction patterns of  $\text{Rb}_4\text{O}_6$  and  $\text{Cs}_4\text{O}_6$  at 300 K (black). The gray curves show the differences between the observed data and the Rietveld refinements.

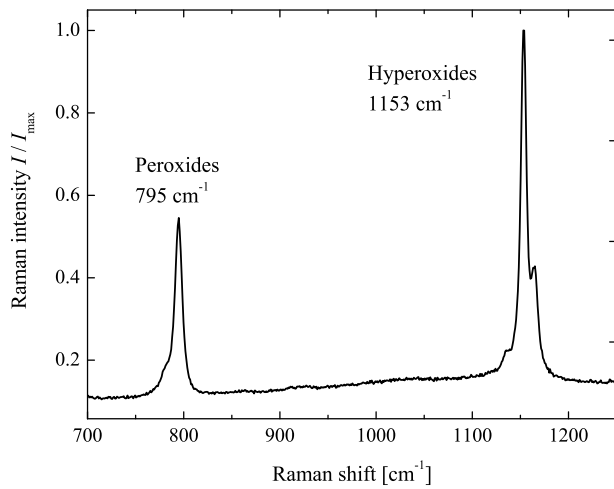


FIG. 3: (Color online) Raman spectrum of  $\text{Rb}_4\text{O}_6$ . The peak at  $795 \text{ cm}^{-1}$  corresponds to the stretching vibration of the peroxide anions and the peak at  $1153 \text{ cm}^{-1}$  to the stretching vibration of the hyperoxide anions.

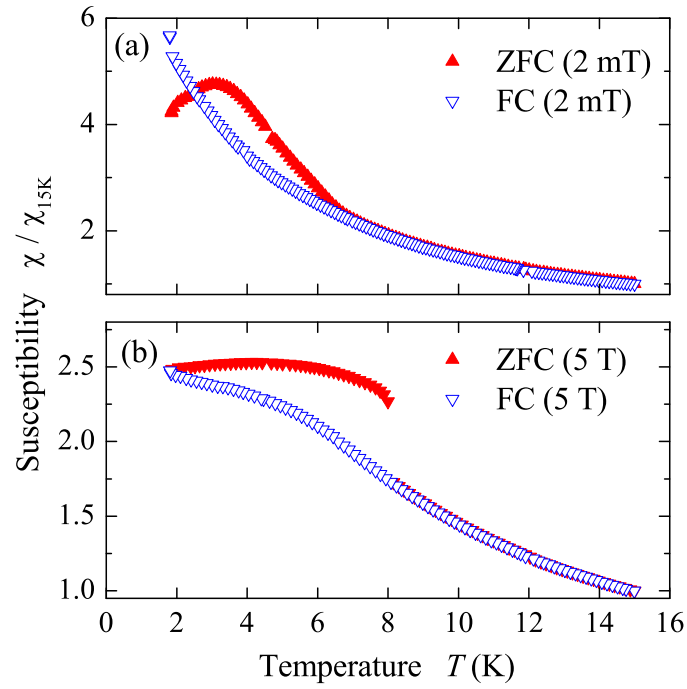


FIG. 4: (Color online) Shown is the temperature dependent magnetic susceptibility of  $\text{Cs}_4\text{O}_6$ . The low-temperature behavior is shown in (a) and (b) for induction fields of 2 mT and 5 T, respectively. (All values are normalized by the value of the susceptibility at 2 K.)

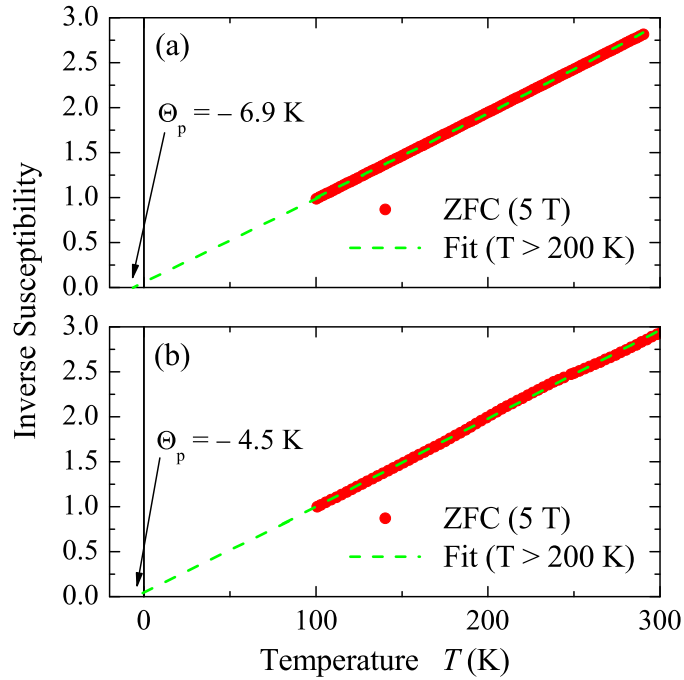


FIG. 5: (Color online) Curie-Weiss-Fits of  $\text{Rb}_4\text{O}_6$ <sup>15</sup> and  $\text{Cs}_4\text{O}_6$ . The data of  $\text{Rb}_4\text{O}_6$  are shown in (a) and the data of  $\text{Cs}_4\text{O}_6$  are shown in (b). The dashed lines represent a Curie-Weiss-Fit in the temperature region above 200 K. (All values are normalized by the values of the inverse susceptibilities at 100 K.)

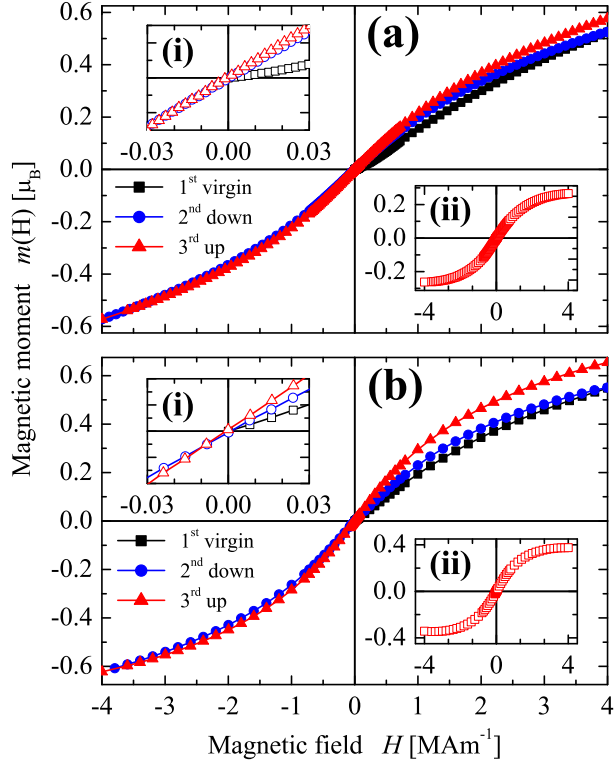


FIG. 6: (Color online) Field dependent magnetization of  $\text{Rb}_4\text{O}_6$  and  $\text{Cs}_4\text{O}_6$  at  $T = 2$  K. Shown are three magnetization cycles as a function of applied  $H$ : virgin ( $0 \rightarrow +H_{max}$ ), down ( $+H_{max} \rightarrow -H_{max}$ ), and up ( $-H_{max} \rightarrow +H_{max}$ ). The insets (i) show in detail the magnetization close to the origin. The insets (ii) show the remaining Langevin functions after subtracting the linear paramagnetic correction.



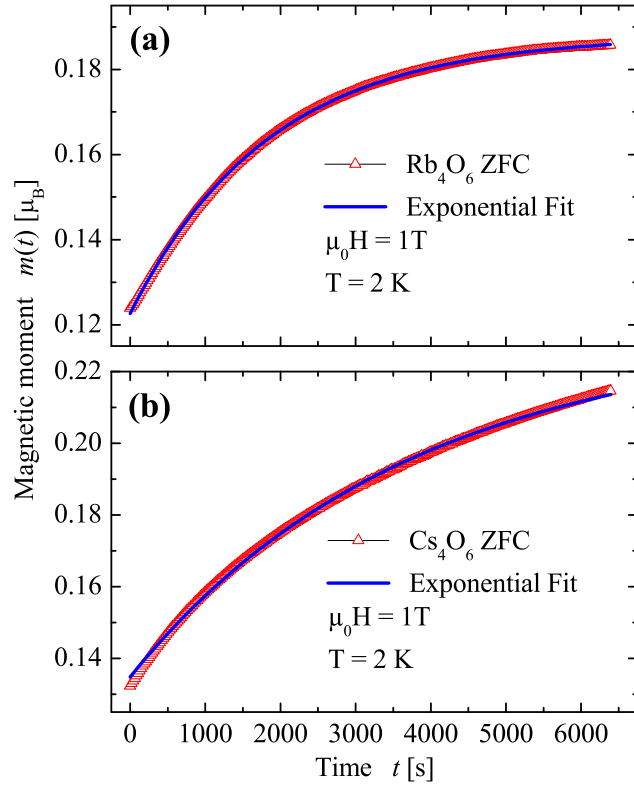


FIG. 7: (Color online) Time dependent magnetizations of  $\text{Rb}_4\text{O}_6$  and  $\text{Cs}_4\text{O}_6$  in induction fields of  $\mu_0 H = 1$  T are shown. The solid lines are the result of exponential fits.

TABLE I: Atomic parameters for  $\text{Rb}_4\text{O}_6$  and  $\text{Cs}_4\text{O}_6$ .

a) In the cubic space group  $I\bar{4}3d$  (no. 220) all alkali or oxygen atoms are equivalent.  $q = d/(2a)$  is the relative position parameter of the oxygen atoms that depends on the bond length  $d$  of the dioxygen anions and the lattice parameter  $a$ .

b) In space group  $I2_12_12_1$  (no. 24) each pair  $\text{O}^{ij}$  ( $i = 1, 2, 3, j = 1, 2$ ) forms one set of  $\text{O}_2$  anions. The centers of these anions are located at  $(7/8, 0, 1/4)$ ,  $(1/4, 7/8, 0)$ , and  $(0, 1/4, 7/8)$ .  $q_1$  and  $q_2$  (for values see Table II) are the relative position parameters of the peroxide and hyperoxide anions, respectively. All permutations of  $q_1$  and  $q_2$  lead to the same structure.

Atom	Site	x	y	z
$I\bar{4}3d$				
AM	16c	t	t	t
O	24d	$3/8 - q$	0	3/4
Rb	16c	1.054696(50)	1.054696(50)	1.054696(50)
O	24d	1.20206(36)	0	3/4
Cs	16c	0.946544(45)	0.946544(45)	0.946544(45)
O	24d	0.55065(49)	0	3/4
$I2_12_12_1$				
AM <sup>1</sup>	8d	$1/4 - t$	$1/4 - t$	$1/4 - t$
AM <sup>2</sup>	8d	$1/2 - t$	$1/2 - t$	$1/2 - t$
O <sup>11</sup>	4a	$7/8 - q_2$	0	1/4
O <sup>12</sup>	4a	$7/8 + q_2$	0	1/4
O <sup>21</sup>	4b	1/4	$7/8 - q_2$	0
O <sup>22</sup>	4b	1/4	$7/8 + q_2$	0
O <sup>31</sup>	4c	0	1/4	$7/8 - q_1$
O <sup>32</sup>	4c	0	1/4	$7/8 + q_1$

TABLE II: Structural parameters for the alkali sesquioxides  $AM_4O_6$ .

Cs data from<sup>11</sup>; Rb data from<sup>8,13</sup> for powder XRD (pd), single crystal (sc) XRD and powder neutron diffraction (nd).  $q = d/(2a)$  is the mean parameter from XRD measurements,  $q_2$  and  $q_1$  are the parameters calculated for  $O_2^-$  and  $O_2^{--}$  ions, respectively (see text).

AM	$a$ [Å]	$t$	$d$ [Å]	$q$	$q_2$	$q_1$	method
Rb	9.3242	0.0545	1.3426	0.072			pd
Rb (295 K)	9.3327	0.05411	1.3234	0.0709			sc
Rb (213 K)	9.2884	0.05377	1.3115	0.0706	0.0721	0.0829	sc
Rb (5 K)	9.2274	0.05395	1.363	0.0738	0.0726	0.0834	nd
Cs	9.86	0.054			0.068	0.078	pd